

## Thermal and Flammability Studies of Poly(vinyl alcohol) Composites Filled with Sodium Hydroxide

Sanjiv Arora, Mahender Kumar, Mahesh Kumar

Department of Chemistry, Kurukshetra University, Kurukshetra-136119, Haryana, India

Correspondence to: S. Arora (E-mail: sanjivkuk@yahoo.co.in)

**ABSTRACT:** Poly(vinyl alcohol) (PVA) is a polymer of great value due to its wide spread applications. The present article describes the effect of sodium hydroxide on the flammability, thermal degradation, and tensile strength properties of PVA. The PVA/sodium hydroxide composite films at different loading levels of sodium hydroxide, i.e., 0.5, 1, 2, 3, and 4.5 wt % were prepared by solution casting technique. Dynamic thermogravimetry was used to study the thermal degradation behavior of samples at four different linear heating rates, i.e., 2.5, 5, 10, and 20 °C min<sup>-1</sup> under nitrogen atmosphere. The degradation activation energy values were calculated using reliable and preferred multiple-heating rate methods. Limiting oxygen index (LOI) and UL 94 tests were carried out to check the flammability behavior of the samples. The presence of sodium hydroxide in PVA brought significant changes in the thermal and flammability performance. PVA/sodium hydroxide samples though showed lower initial decomposition temperature, but overall more thermal stability results as evidenced from the higher activation energy and char residue values. LOI and UL 94 tests indicate that sodium hydroxide greatly enhanced the flame retardancy of PVA/sodium hydroxide films. Based on the thermal and flammability level, the optimum concentration of sodium hydroxide is worked out. © 2012 Wiley Periodicals, Inc. *J. Appl. Polym. Sci.* 000: 000–000, 2012

**KEYWORDS:** activation energy; biodegradable; blending; thermogravimetric analysis (TGA); flame retardance

Received 14 March 2011; accepted 13 March 2012; published online 00 Month 2012

DOI: 10.1002/app.37705

### INTRODUCTION

Poly(vinyl alcohol) (PVA) has received great attention for being an inexpensive, biodegradable, and environmental friendly polymeric material. It is widely used because of many desirable characteristics such as good film forming capability, flexibility, non-toxic, binding properties, and high tensile strength, etc.<sup>1–3</sup> However, PVA is a highly flammable polymeric material and needs to be made a better flame-retarding one.

Halogen-based additives are among the most effective and widely used flame retardants (FR) for the natural and synthetic polymers. But now-a-days their use as FR is discouraged for being non eco-friendly.<sup>4–6</sup> Therefore, developing halogen-free FR systems has become an attractive and growing field of interest. Another important aspect to keep in mind is that the mechanical properties of the polymer remain largely unaffected while translating it into a non-flammable one. For achieving a good FR level, one has to add higher FRs loadings to the polymer, causing significant decrease in the mechanical properties of the polymer.<sup>7,8</sup> Wu et al.<sup>9</sup> have already reported the use of microencapsulated ammonium polyphosphate for preparing flame-retarded PVA/starch thermoplastic composites. However, microencapsula-

tion of ammonium polyphosphate using melamine-formaldehyde prepolymer is not considered eco-friendly. Wang et al.<sup>10</sup> have prepared novel intumescent flame retardant system containing metal chelates for PVA and reported limiting oxygen index (LOI) value of ~ 34% at a total FR loading of 15 wt %. Zhao et al.<sup>11</sup> have also studied the effect of ammonium polyphosphate and double layered hydroxides on the flammability properties of PVA. It was thought that the addition of sodium hydroxide to PVA may possibly decrease the flammability of PVA in line with the work of Mostashari et al.,<sup>12</sup> using a small deposition of sodium hydroxide on cotton fabric to make it flame-resistant after drying and thus the method seem to be attractive in terms of easy process and low cost of sodium hydroxide at the same time.

Dynamic thermogravimetry (TG), derivative thermogravimetric (DTG), LOI, and Underwriter's Laboratory test (UL 94) are the most frequently used techniques to examine the thermal and flammability behavior of polymeric materials.<sup>13</sup> TG has the main advantage in respect of the high reproducibility of results in dynamic style for calculating precise kinetic parameters. It is worth noting that kinetic study is useful in predicting the mechanism of thermal degradation process.<sup>14</sup> This, in turn, may help to study the

© 2012 Wiley Periodicals, Inc.

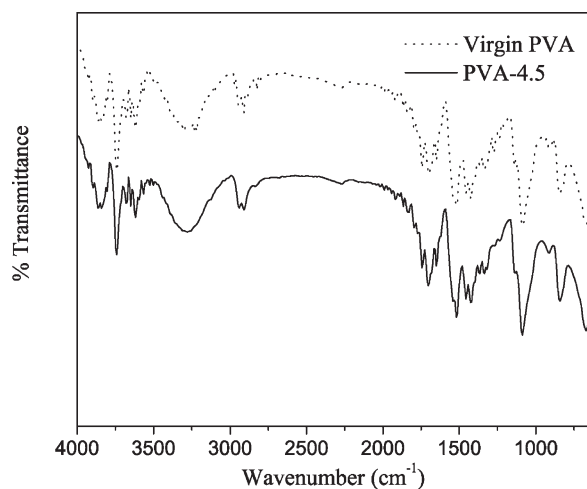


Figure 1. FTIR spectra of virgin PVA and PVA-4.5.

effect of sodium hydroxide as FR on PVA. However, the calculation of kinetic parameters using single heating rate methods is facing disapproval due to problematic procedures and unreliable results.<sup>13,15</sup> Consequently, the use of multiple-heating rate methods, e.g., Kissinger,<sup>16</sup> Friedman,<sup>17</sup> Ozawa–Flynn–Wall (O-F-W),<sup>18,19</sup> and Coats–Redfern (modified)<sup>20,21</sup> is opted.

In the present investigation, PVA/sodium hydroxide blends were prepared via solution casting method. The thermal degradation behavior of the samples was studied using dynamic TG/DTG analyses followed by multiple-heating rate kinetics. Flammability behavior of composite films was checked by reliable laboratory methods viz. LOI and UL 94. Tensile properties of composite films were also tested using Universal testing machine.

## EXPERIMENTAL

### Preparation of PVA/Sodium Hydroxide Blends

A series of PVA/sodium hydroxide films were prepared by solution casting method varying the contents of sodium hydroxide from 0 to 4.5 wt %. PVA was dissolved in hot water at 80°C, while sodium hydroxide in deionized water to form solution. PVA and sodium hydroxide solutions were then mixed and

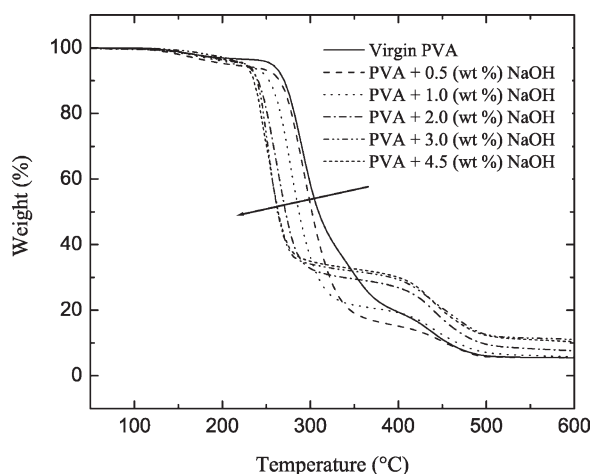


Figure 2. TG thermograms for PVA/sodium hydroxide composites at a heating rate of 20 °C min<sup>-1</sup>.

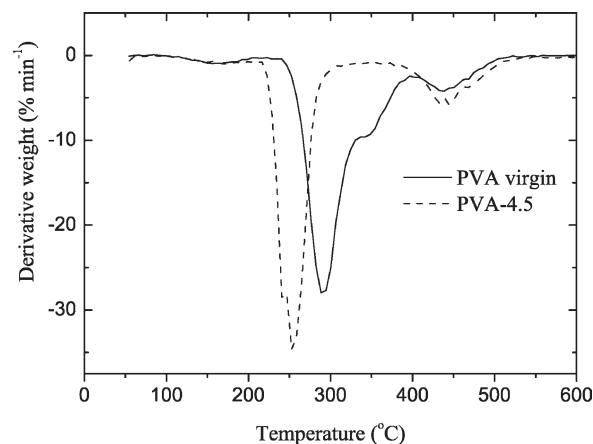


Figure 3. DTG thermograms of PVA and PVA-4.5 at a heating rate of 20 °C min<sup>-1</sup>.

stirred for 2 h. The solution was finally cooled to ambient temperature, and films were cast into clean poly(propylene) dishes. The composite films were dried in vacuum oven at 60°C for 12 h in order to remove moisture content, which were named according to the percentage loading level, i.e., PVA, PVA-0.5, PVA-1, PVA-2, PVA-3, and PVA-4.5 corresponding to 0, 0.5, 1, 2, 3, and 4.5 wt %.

### Fourier Transform Infrared Spectroscopy

Fourier transform infrared spectroscopy (FTIR) spectra of PVA and PVA-4.5 were recorded in transmission mode with a MB-3000 ABB Spectrometer over the range 4000–650 cm<sup>-1</sup>.

### Limiting Oxygen Index

LOI values of the samples were measured according to ASTM D2863 using S.A. Associate's PLATON oxygen index apparatus. The specimen used for the test was of 100 × 6 × 2 mm<sup>3</sup> dimensions. LOI values were calculated according to the following equation:

$$\text{LOI}(\%) = [\text{O}_2]/([\text{O}_2] + [\text{N}_2])$$

where [O<sub>2</sub>] and [N<sub>2</sub>] represent the oxygen and nitrogen concentrations, respectively.

### UL 94 Testing

The flame spread rate of all the samples was investigated by the horizontal burning test (HB) according to the UL 94 test standards. The specimen used for the test was of 125 × 13 × 2 mm<sup>3</sup> dimensions. Five tests were conducted for each sample. The flame spread or burning rate (mm min<sup>-1</sup>) was calculated using the following equation:

$$\text{Flame spread rate} = 100/(t - t_1)$$

where  $t_1$  is the burning time from the beginning to 25 mm, and  $t$  is the burning time from the beginning to 100 mm. The flame is applied to the free end of the specimen for 30 s. The time for the flame front to move between the benchmarks is measured. Sample is classified as HB rating if the burning rate does not

**Table I.** TG/DTG Data for PVA/Sodium Hydroxide Composites at a Heating Rate of 20 °C min<sup>-1</sup>

Sample	First stage					Second stage			
	T initial (°C)	Tm1 (°C)	T term (°C)	PWHL (min)	WL (at 260°C) (%)	T initial (°C)	Tm2 (°C)	T term (°C)	Char residue at 600°C (%)
PVA	238.3	289.0	390.0	1.9	5.7	400.6	439.0	517.0	5.5
PVA-0.5	237.1	294.2	370.0	2.3	8.3	399.1	443.0	516.5	5.5
PVA-1	231.8	278.8	342.0	1.9	14.0	398.3	441.0	520.0	5.7
PVA-2	222.5	263.1	325.0	1.8	32.6	400.0	441.5	516.1	7.5
PVA-3	225.1	256.6	305.0	1.5	40.5	392.0	437.0	520.0	9.5
PVA-4.5	217.3	254.5	303.3	1.5	45.3	391.5	439.8	525.0	10.3

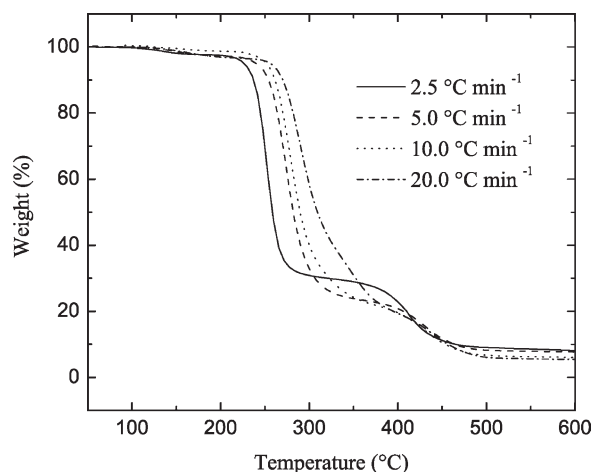
exceed 75 mm min<sup>-1</sup> or sample gets self-extinguished before 100 mm benchmark.

### Tensile Testing

The tensile properties of the PVA films are measured with a Universal testing machine. The test specimens were in the form of dumbbells according to ASTM D 638 and conditioned at 50% relative humidity, 25°C for 24 h. The crosshead speed was 10 mm min<sup>-1</sup>. The reported data are the average of five measurements.

### Thermal Analysis

Thermograms of the samples were observed under a flowing nitrogen atmosphere (20 mL min<sup>-1</sup>) at four different linear heating rates, i.e., 2.5, 5, 10, and 20 °C min<sup>-1</sup> using Perkin Elmer, Diamond thermogravimetric/differential thermal analyzer. The instrument was calibrated before recording thermograms. Dried Alumina powder (Al<sub>2</sub>O<sub>3</sub>) was employed as reference material using ceramic sample holder for taking thermograms. In order to ensure the uniformity of temperature of the sample and good reproducibility, small amounts were taken. To verify the reproducibility of obtained weight loss curve, two sample runs were performed under the same experimental conditions for each sample at the chosen heating rates. Activation energies were calculated with a specially designed program in MS-Excel, which takes specific TG and DTG records from the Pyris manager software.

**Figure 4.** TG thermograms for virgin PVA at four linear different heating rates.

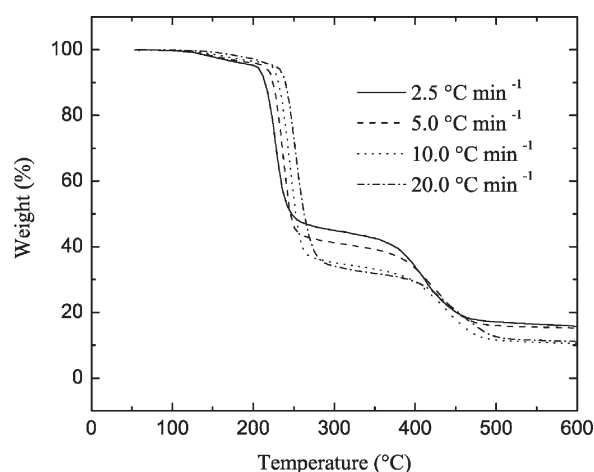
## RESULTS AND DISCUSSION

### FTIR Studies

Figure 1 shows the FTIR spectra of virgin PVA and PVA-4.5. Significantly, both PVA and PVA-4.5 have displayed alike FTIR spectra. A number of bands observed at 3850, 3742, 3600, and 3280 cm<sup>-1</sup> relate to the O—H stretching from absorbed moisture and intermolecular and intramolecular hydrogen bonds.<sup>22</sup> The vibration bands observed at 2939 and 2908 cm<sup>-1</sup> correspond to stretching C—H from alkyl groups and the peaks at 1744 and 1705 cm<sup>-1</sup> relate to the C=O and C—O stretching from residual acetate groups in PVA. Besides, a shoulder appears at 1650 cm<sup>-1</sup> due to C=C stretching vibration.<sup>23</sup> A set of bands at 1520, 1427, and 1366 cm<sup>-1</sup> owing to C—H/O—H bending and 1088 cm<sup>-1</sup> of C—O—H stretching appeared in PVA and PVA-4.5 samples.<sup>24</sup>

### Thermal Studies Based on TG Data

The TG thermograms of neat PVA and PVA/sodium hydroxide films are shown in Figure 2. TG curves of all the samples showed a slight weight loss around 150°C, which can be attributed to the loss of absorbed water. It is well documented<sup>25–27</sup> that the degradation of PVA obeys two-step mechanism and is confirmed to be a two-step process by the DTG curve (Figure 3). The first step in the weight loss curve results from the dehydration and depolymerization of PVA accompanied by the polyene formation. During the second step, residue of the first stage

**Figure 5.** TG thermograms for PVA-3 at four linear different heating rates.

**Table II.** Kinetic Methods Used in Calculating Activation Energy in This Study

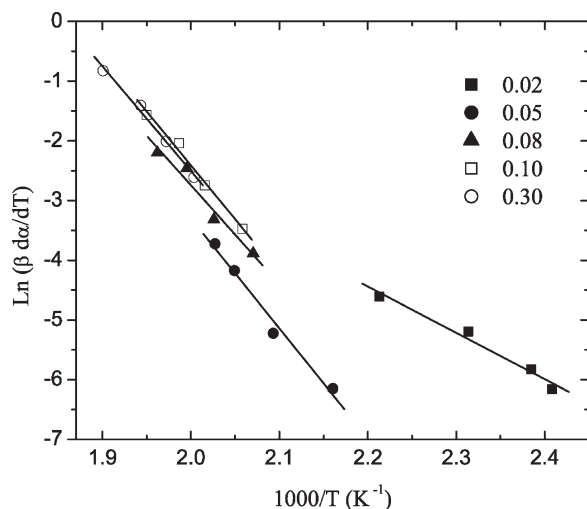
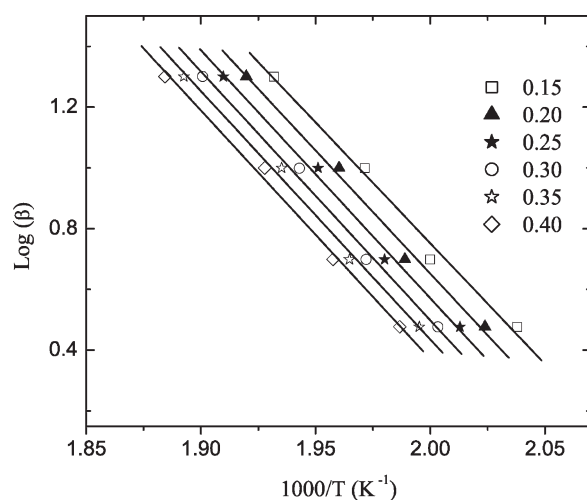
Method	Final equation	Plots
O-F-W	$\log(g(x)) = \log\left(\frac{AE}{R}\right) - \log(\beta) - 2.315 - 0.4567 \frac{E}{RT}$	$\log \beta$ against $1/T$
Kissinger	$\frac{d(\ln(\beta/T_m^2))}{d(1/T_m)} = -\frac{E}{R}$	$\ln(\beta/T_m^2)$ against $1/T_m$
Friedman	$\ln\left(\frac{d\alpha}{dt}\right) = \ln\left(\beta \frac{d\alpha}{dT}\right) = \ln A + n \ln(1-\alpha) - \frac{E}{RT}$	$\ln(\beta(d\alpha/dT))$ against $1/T$
Coats-Redfern (modified)	$\ln\left[\frac{\beta}{T^2(1-\frac{2RT}{E})}\right] = \ln\left[-\frac{AR}{E \ln(1-\alpha)}\right] - \frac{E}{RT}$	$\ln(\beta/T^2)$ against $1/T$

undergoes pyrolysis reactions such as intramolecular cyclization, producing some organic volatiles.<sup>26</sup> It can be seen from Figures 2 and 3 that the presence of sodium hydroxide changes the degradation behavior of PVA composites. In the first step, initial degradation temperature ( $T$  initial) and the temperature at which maximum weight loss occur ( $Tm1$ ) decrease by  $\sim 21$  and  $34^\circ\text{C}$ , respectively, for PVA-4.5 as compared to virgin PVA (Table I).

In order to show how sodium hydroxide has decreased the time period of dehydration step (first step); a parameter named PWHL (DTG peak width at half length or height) was calculated. Noticeably, PWHL decrease from 1.9 for PVA to a minimum of 1.5 min for PVA-4.5 (except 0.5 wt % loading). Hence, the presence of sodium hydroxide causes an early dehydration of PVA and also shrinks the dehydration process to shorter time duration. In addition, the value of the percentage weight loss ( $W_L$ ) at  $260^\circ\text{C}$  (middle point of first step in case of PVA-4.5) shows a large increase, i.e., for virgin matrix  $W_L$  is only 5.7 whereas for 4.5 wt % loading it is 45.3. It means large amounts

of dehydration products mainly water are available at comparatively lower temperatures which may possibly dissipate the heat for its evaporation, and may further dilute the flammable gases produced during degradation.<sup>12</sup> Importantly, weight (%) left after the first stage is highest for PVA-4.5 and the specific order is: PVA-4.5 > PVA-3 > PVA-2 > PVA-1 = PVA > PVA-0.5 indicating PVA/sodium hydroxide samples (except PVA-0.5) are thermally more stable at elevated temperatures as compared to virgin PVA (Figure 2). Further, there is not much difference between the thermal profiles of PVA-3 and PVA-4.5 (Figure 2 and Table I). It can be understood that 3% is the optimum level of sodium hydroxide.

After the completion of first degradation step, weight (%) remains almost constant till the commencement of second degradation stage. The second stage starts at  $400.6$  and  $391.5^\circ\text{C}$  for PVA and PVA-4.5, respectively. Noticeably, the second stage temperature parameters (second maxima in DTG curve ( $Tm2$ ) and degradation termination temperature ( $T$  term)) varied only slightly on adding sodium hydroxide to PVA, which is indicative

**Figure 6.** Iso-conversional Friedman plots for PVA-3.**Figure 7.** Iso-conversional O-F-W plots for PVA-3.

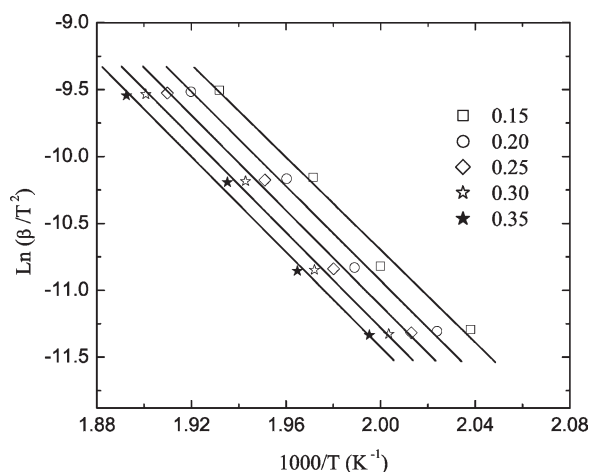


Figure 8. Iso-conversional Coats-Redfern plots for PVA-3.

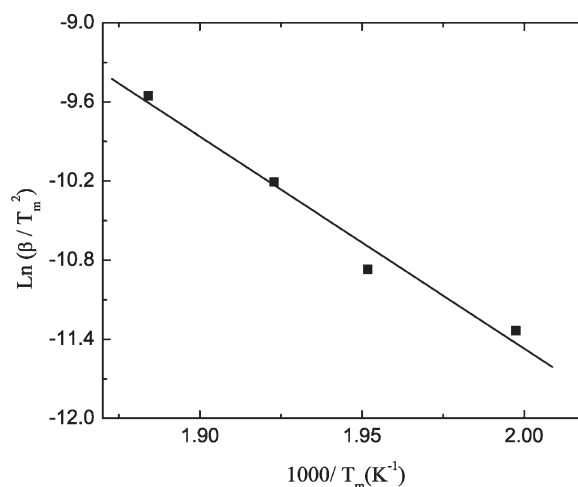


Figure 9. Kissinger plot for PVA-3.

of low impact of sodium hydroxide on pyrolysis reaction occurring during second stage<sup>26</sup> (Table I). The value of percentage weight left at 600°C increases from 5.5 (PVA) to 10.3 (PVA-4.5) which means sodium hydroxide does not bring any major change in residual char and simply adds to the final weight at 600°C. This is in agreement with the work reported earlier.<sup>12,28</sup> Therefore, it may be concluded here that the presence of sodium hydroxide causes an early dehydration process, while the pyrolysis reactions remain unaffected.

### Kinetic Studies

As discussed above in the previous section that the 3 wt % loading is the optimum level, therefore, PVA and PVA-3 were chosen for further comparative kinetic studies. In order to get a broad view of degradation activation energy variation with degree of conversion, four different multiple heating rate non-

isothermal methods were used. Thermograms were observed at four different linear heating rates and are shown in Figures 4 and 5, as expected the slower heating rate gives better differentiation of the degradation process and provides an early start to it. A reduced thermal lag is the core mechanism responsible for a better differentiation.

The main equations of the kinetic methods used in studying the thermal degradation of PVA samples are summarized in Table II. In these equations,  $\beta$  is the heating rate,  $T_m$  is the temperature at maximum rate of weight loss,  $n$  is the reaction order,  $R$  is the universal gas constant,  $A$  is the pre-exponential factor,  $\alpha$  is the degree of conversion, and  $E$  is the activation energy.

The plots of iso-conversional Friedman, O-F-W, and modified Coats-Redfern methods show a general trend of activation

Table III. The Values of Degradation Activation Energy at Varying Degree of Conversions

Degree of conversion	Activation energy (kJ mol <sup>-1</sup> )					
	PVA virgin			PVA-3		
	O-F-W	Coats-Redfern (modified)	Friedman	O-F-W	Coats-Redfern (modified)	Friedman
0.05	122.5	120.3	124.0	-	-	153.2
0.06	123.2	121.0	123.7	139.6	138.7	-
0.07	123.2	120.9	124.9	144.8	144.0	-
0.08	123.3	120.9	124.5	140.2	139.1	137.6
0.09	123.4	121.1	118.5	140.0	139.0	150.5
0.10	123.0	120.6	112.9	141.2	140.3	149.6
0.15	120.5	117.2	99.1	144.7	143.9	155.2
0.20	116.8	113.9	90.6	147.4	146.7	151.9
0.25	113.3	110.1	82.5	148.5	147.8	150.6
0.30	109.7	106.4	74.6	149.1	148.3	145.8
0.35	106.2	102.6	71.5	148.7	147.9	148.8
0.40	102.9	99.1	61.5	148.9	147.9	154.1
0.45	99.0	95.0	57.2	149.8	149.0	168.2
0.50	94.6	90.6	47.5	152.9	152.1	-
0.55	89.7	85.0	39.5	161.2	160.4	-
0.60	83.3	78.2	35.9	-	-	-

**Table IV.** LOI and UL 94 Test Results of PVA/Sodium Hydroxide Composites

Sample	LOI (%)	UL 94 testing		
		Flame spread rate (mm min <sup>-1</sup> )	Burning character	HB test rating
PVA virgin	20.5	81.0	Dripping, small swelling	Fail
PVA-0.5	21.1	77.6	Less dripping, small swelling	Fail
PVA-1.0	23.5	51.3	No or less dripping, swelling	Pass
PVA-2.0	25.3	37.6	No or less dripping, swelling	Pass
PVA-3.0	26.8	28.0	Swelling, no dripping	Pass
PVA-4.5	27.2	27.8	Swelling, no dripping	Pass

energy. To illustrate, the Friedman plot for PVA-3 (Figure 6), while Figures 7 and 8 are due to the specific results of application of O-F-W and modified Coats-Redfern methods, respectively. Figure 9 shows the linear plots of  $\ln(\beta/T_m^2)$  against  $1/T_m$  for PVA-3 employing Kissinger method. The evaluated degradation activation energies thus obtained at varying degrees of conversion of the samples are summarized in Table III.

It is noticed that the values by Kissinger's method are holistically lower than the ones by iso-conversional methods.<sup>29</sup> However, the results calculated by these methods are showing a general trend of activation energy in going either from virgin PVA to PVA-3 or moving from lower to higher degree of conversions for each sample.

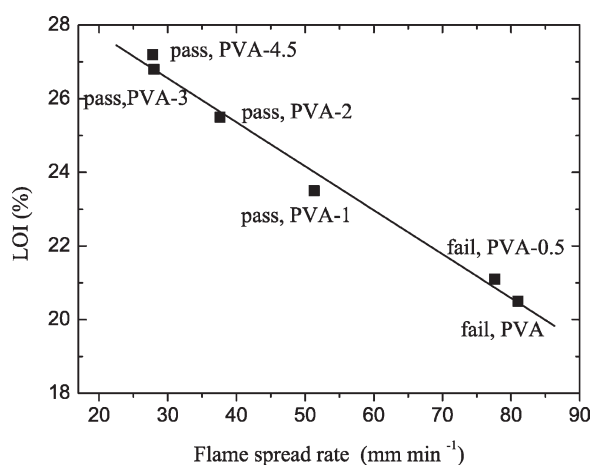
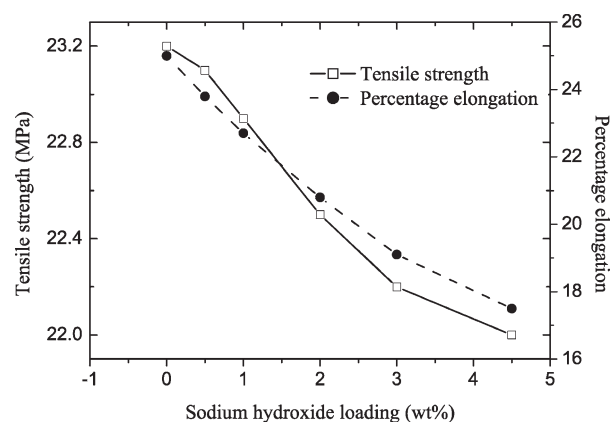
In case of virgin PVA, iso-conversional methods, i.e., Friedman, Coats-Redfern, and O-F-W produce almost the same value of initial degradation activation energy in the range 120–124 kJ mol<sup>-1</sup>. The values found by these methods remain almost constant upto  $\alpha = 0.09$ , and thereafter show a regular decrease with increase in degree of conversion. However, Friedman's method gives relatively large decrease in values of activation energy; for example the value by Friedman is 35.9 at  $\alpha = 0.6$  whereas it is 78.2 and 83.3 kJ mol<sup>-1</sup> by Coats-Redfern and O-F-W, respectively.

The initial degradation activation energy values for PVA-3 are larger as compared to PVA and increase on moving towards higher degrees of conversion. In general, the values of activation energy by all the methods are comparatively larger for the PVA-3. For instance, the values calculated using Friedman, Coats-

Redfern, and O-F-W methods at 0.1 degree of conversion, are 112.9 (149.6), 120.6 (140.3), and 123.0 (141.2) kJ mol<sup>-1</sup>, for the samples PVA (PVA-3), respectively. In addition, activation energy calculated using Kissinger method shows similar trend, i.e., first stage degradation activation energy of PVA-3 (133 kJ mol<sup>-1</sup>) is higher than those for virgin PVA (113 kJ mol<sup>-1</sup>). Higher  $E$  for the initial degradation for PVA-3 may be attributed to the early (low temperature) formation of large amounts of dehydration products mainly water as deduced from TG data.<sup>12</sup> It is anticipated that PVA-3 might have to consume extra energy for vaporization of water besides that required for the degradation process resulting in overall higher stability. Evidently, almost double  $E$  values at  $\alpha = 0.55$  are obtained for PVA-3 as compared to PVA. It indicates higher thermal stability of PVA-3 than virgin PVA at higher conversions and as a result thereof flame retardancy may increase. Similar results are obtained from TG data as already discussed above; hence, showing a good correlation between TG and kinetic studies. Perhaps the degradation activation energy measured can be helpful to understand the role of sodium hydroxide as a flame retardant and would also give new directions for further investigation.

### Flammability Studies

LOI values and UL 94 results of PVA and PVA/sodium hydroxide films are shown in Table IV. It has been noted while UL 94 testing that PVA films with loading level greater than 1, burn without dripping. This behavior is different from neat PVA which drips badly. Virgin PVA is highly combustible and its

**Figure 10.** Correlation plot between LOI values and flame spread rates.**Figure 11.** Effect of sodium hydroxide loading on tensile properties of PVA/sodium hydroxide composites.

LOI value is 20.5%. It can be noticed from the table that the LOI values of PVA/sodium hydroxide films increase with increase in sodium hydroxide content. LOI value of PVA-3 is as high as 26.8% which clearly point towards lower flammability of PVA-3 than the neat PVA. Further addition of sodium hydroxide to PVA-3, does not bring any significant change in LOI and flame spread rate. These findings match well with TG results; for example, TG curves and LOI values of PVA-3 and PVA-4.5 are just overlapping. Lower flammability of PVA/sodium hydroxide samples are in accordance with the conclusion drawn from activation energy values as stated already. Also, flame spread rates calculated by UL 94 testing are in line with LOI values. To correlate the UL 94 results with LOI values, a graph between them was drawn as shown in Figure 10. It indicates a good correlation characterized by high value of regression coefficient close to 1.

PVA film swells on heating owing to the elimination of water vapors.<sup>26</sup> It is seen that swelling is more pronounced in case of PVA/sodium hydroxide composites. This is in agreement with the TG results which concluded that sodium hydroxide gives an early start to the dehydration process and produces more water vapors than neat PVA. This extra water vapors possibly dilutes the fuel gases produced during the combustion resulting in increase of LOI value.<sup>12,30</sup> After swelling, decomposition of PVA results in yellow mass which changes to a black residue. It has been noticed that the sodium hydroxide containing films result into a rigid and more expanded char layer which is different from neat PVA thereby preventing the heat transfer and cut oxygen supply, thus delays the spread of flame.<sup>12</sup> This protective layer possibly consists of sodium oxide produced from the decomposition of sodium hydroxide at elevated temperatures which may act as thermal barrier.<sup>28,30,31</sup> Hence, the mechanism of flame retardancy imparted by sodium hydroxide may be understood by gas dilution theory as well as barrier theory.

### Tensile Properties

Tensile strength and percentage elongation were measured for the PVA/sodium hydroxide composite films as shown in Figure 11. Tensile strength values of composites showed a slight but regular decrease with increase in sodium hydroxide loading. It is assumed that sodium as well as hydroxide ions may come in between the PVA chains resulting in lower intermolecular hydrogen bonding and subsequently, lower tensile strength. Composite films become brittle on adding sodium hydroxide resulting in decrease of elongation (%).

### CONCLUSION

The effect of sodium hydroxide on the thermal stability and flame retardancy of PVA was studied using TG/DTG, kinetics, LOI, and UL 94 techniques. Tensile properties of composites however, show a slightly declining trend on increasing sodium hydroxide loading. TG/DTG experiments explained that the sodium hydroxide causes early release of water from PVA and the substrate might have to consume extra energy for vaporization of water besides the energy required for the degradation process. Degradation activation energy data too supports the above statement. PVA/sodium hydroxide composites exhibit enhanced flame retardancy over virgin PVA as indicated by LOI and UL

94 tests. It is thought that the fuel gas dilution by water vapors is more pronounced for PVA/sodium hydroxide composites as revealed by TG studies. In addition, thermal barrier caused by stable sodium oxide layer formed on decomposition at high temperatures can be responsible for improved flame retardancy of PVA/sodium hydroxide films. It is revealed that 3% loading is the optimum level of sodium hydroxide for effecting improvement in flame retardancy of PVA. Thus, sodium hydroxide can be used to prepare low cost and low flammable PVA/sodium hydroxide composites which compare favorably well with the existing ones in use.

### ACKNOWLEDGMENTS

Mahender Kumar is grateful to Kurukshetra University, Kurukshetra for awarding University Research Scholarship and Mahesh Kumar is thankful to Council of Scientific and Industrial Research, New Delhi, India for providing Senior Research Fellowship. Authors are also thankful to Mr. J.K. Bihani (Galaxy Plywood Industries, Yamunanagar) for his support. Thanks are due to Prof. Lajpat Rai Kakkar for going through the manuscript.

### REFERENCES

1. Chabba, S.; Netravali, A. N. *J. Mater. Sci.* **2005**, *40*, 6275.
2. Sreedhar, B.; Sairam, M.; Chattopadhyay, D. K.; Rathnam, P. A. S.; Rao, D. V. M. *J. Appl. Polym. Sci.* **2005**, *96*, 1313.
3. Nishiyama, M.; Yamamoto, R.; Hoshiro, H. In 10th International Inorganic-Bonded Fiber Composites Conference, São Paulo, Brazil, **2006**; p 120.
4. Wang, X.; Wu, L.; Li, J. *J. Therm. Anal. Calorim.* **2011**, *103*, 741.
5. Pal, K.; Rastogi, J. N. *J. Appl. Polym. Sci.* **2004**, *94*, 407.
6. World Health Organization. EHC-197, Flame-Retardant: A General Introduction, International Program on Chemical Safety; World Health Organization: Geneva, Switzerland, **1997**.
7. Huang, H.; Tian, M.; Yang, J.; Li, H.; Liang, W.; Zhang, L.; Li, X. *J. Appl. Polym. Sci.* **2008**, *107*, 3325.
8. Chen, X.; Yu, J.; Guo, S. *J. Appl. Polym. Sci.* **2006**, *102*, 4943.
9. Wu, K.; Hu, Y.; Song, L.; Lu, H.; Wang, Z. *Ind. Eng. Chem. Res.* **2009**, *48*, 3150.
10. Wang, D. L.; Liu, Y.; Wang, D.-Y.; Zhao, C. X.; Mou, Y.-R.; Wang, Y.-Z. *Polym. Degrad. Stab.* **2007**, *92*, 1555.
11. Zhao, C. X.; Liu, Y.; Wang, D.-Y.; Wang, D. L.; Wang, Y.-Z. *Polym. Degrad. Stab.* **2008**, *93*, 1323.
12. Mostashari, S. M.; Nia, Y. K.; Fayyaz, F. *J. Therm. Anal. Calorim.* **2008**, *91*, 237.
13. Arora, S.; Kumar, M.; Kumar, M. *J. Therm. Anal. Calorim.*, **2012**, *107*, 1277.
14. Arora, S.; Lal, S.; Kumar, S.; Kumar, M.; Kumar, M. *Arch. Appl. Sci. Res.* **2011**, *3*, 188.
15. Vyazovkin, S. *Thermochim. Acta* **2000**, *355*, 155.
16. Kissinger, H. E. *Anal. Chem.* **1957**, *29*, 1702.
17. Friedman, H. L. *J. Polym. Sci. Part C* **1964**, *61*, 183.

18. Ozawa, T. *Bull. Chem. Soc. Jpn.* **1965**, 38, 1881.
19. Flynn, J. H.; Wall, L. A. *Polym. Lett.* **1966**, 4, 323.
20. Burnham, A. K.; Braun, R. L. *Energy Fuels* **1999**, 13, 1.
21. Kofstad, P. *Nature* **1957**, 179, 1362.
22. Peresin, M. S.; Habibi, Y.; Zoppe, J. O.; Pawlak, J. J.; Rojas, O. J. *Biomacromolecules* **2010**, 11, 674.
23. Chen, Y.; Sun, Z.; Yang, Y.; Ke, Q. *J. Photochem. Photobiol. A: Chem.* **2001**, 142, 85.
24. Nath, D. C. D.; Bandyopadhyay, S.; Boughton, P.; Yu, A.; Blackburn, D.; White, C. *J. Mater. Sci.* **2010**, 45, 2625.
25. Shie, J.-L.; Chen, Y.-H.; Chang, C.-Y.; Lin, J.-P.; Lee, D.-J.; Wu, C.-H. *Energy Fuels* **2002**, 16, 109.
26. Gilman, J. W.; Vanderhart, D. L.; Kashiwagi, T. *Fire and Polymers II: Material and Test for Hazard Prevention*; ACS Symposium Series 599; American Chemical Society: Washington, DC, **1994**.
27. Thomas, P. S.; Guerbois, J.-P.; Russell, G. F.; Briscoe, B. J. *J. Therm. Anal. Calorim.* **2001**, 64, 501.
28. Yurkinskii, V. P.; Firsova, E. G.; Proskura, S. A. *Russ. J. Appl. Chem.* **2005**, 78, 360.
29. Arora, S.; Kumar, M.; Dubey, G. P. *J. Energy Inst.* **2009**, 82, 138.
30. Levan, S. L. *Chemistry of Fire Retardancy*; American Chemical Society: Washington, DC, **1984**; Chapter 14, p 531.
31. Bourbigot, S.; Duquesne, S. *J. Mater. Chem.* **2007**, 17, 2283.